Mechanisms of the Transition Metal-Mediated Hydroarylation of Alkynes and Allenes

Elena Soriano*,† and José Marco-Contelles‡

Laboratorio de Resonancia Magnética, Instituto de Investigaciones Biomédicas (CSIC), C/ Arturo Duperier 4, 28029-Madrid, Spain, and Laboratorio de Radicales Libres, IQOG (CSIC), C/ Juan de la Cierva 3, 28006-Madrid, Spain

Received June 19, 2006

We report the theoretical analysis of the mechanism of the intramolecular cyclization of biaryl alkynes and allenes, catalyzed by electrophilic transition metal complexes and soft Lewis acids. These reactions proceed through initial π-complexation of the alkyne or allene moiety, which triggers the nucleophilic attack of the arene via an *endo*- or *exo-dig* pathway in a Friedel−Crafts-type mechanism. In addition, alternative reaction mechanisms have been considered to account for some experimental observations. The computed results over a variety of substrates and catalyst systems agree with experimental evidence and suggest that both structural and electronic effects play a crucial role in the regioselectivity outcome and in the involvement of operative intermediates in the reaction pathway.

1. Introduction

In the last years, the increasing interest in developing more efficient strategies for the synthesis of functionalized polycycles has led to the study and application of a range of new catalyst systems able to catalyze C−C formation. Transition metal complexes have been shown to perform highly efficient cycloisomerizations of polyunsaturated precursors in a stereocontrolled way, to yield a wide variety of carbo- and heterocyclic compounds.[1] Thus, cycloisomerizations of enynes promoted by electrophilic transition metal complexes have emerged as a powerful synthetic protocol, fully atom economic, which may give rise to important structural motifs in natural products (Scheme 1).[2−5] Remarkably, these processes can selectively afford different cyclic structures depending on the reaction conditions (catalyst system and solvent).

As a part of the broad scope, this flexible protocol has also been applied in the hydroarylation of alkynes to form carbo- and heteroarene derivatives, such as coumarins and quinolinones,

Scheme 1

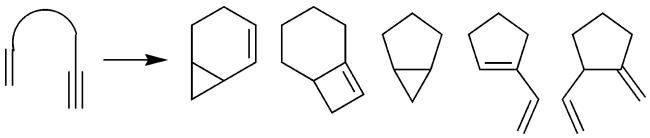

as an alternative to cross-couplings or the Heck reaction.[6] Both inter- and intramolecular processes have been disclosed by various groups. Recently, Fürstner et al. have reported[7] the intramolecular formation of phenantrenes and polycyclic heteroarenes catalyzed by a variety of soft Lewis acids: $PtCl_2$, $AuCl_3$, $GaCl_3$, and $InCl_3$. They found that the regioselectivity for this reaction was dependent on the catalyst system and on the precursor structure (Scheme 2).

The scope of this protocol was also extended to other unsaturated groups acting as electrophiles, by coordination to a electron-deficient metal complex, such as allene. The intramolecular hydroarylation of allenes also revealed a well-defined regioselectivity, which was strongly dependent on the catalyst. Thus, the allene precursor **IV** afforded the phenanthrene framework **V** when Ga(III) and In(III) were employed as catalysts, whereas $PtCl_2$ gave rise to a mixture of isomeric pyrrolo-azepines **VI** and **VII** as major products (Scheme 3). These results suggest a 6-*exo-dig* and 7-*endo-dig* cyclization pathway, respectively.[7c]

These intriguing data and our continuing interest in this field[8] prompted us to perform a detailed computational study on the mechanism of the intramolecular hydroarylation of alkynes and allenes, catalyzed by different catalyst systems.

* To whom correspondence should be addressed. E-mail: esoriano@iib.uam.es.

† Laboratorio de Resonancia Magnética.

‡ Laboratorio de Radicales Libres.

(1) (a) Lloyd-Jones, G. C. *Org. Biomol. Chem.* **2003**, *1*, 215−236. (b) Méndez, M.; Mamane, V.; Fürstner, A. *Chemtracts* **2003**, *16*, 397−425. (c) Aubert, C.; Buisine, O.; Malacria, M. *Chem. Rev.* **2002**, *102*, 813−834.

(2) (a) Bruneau, C. *Angew. Chem., Int. Ed.* **2005**, *44*, 2328−2334. (b) Fürstner, A.; Szillat, H.; Stelzer, F. *J. Am. Chem. Soc.* **2000**, *122*, 6785−6786. (c) Méndez, M.; Muñoz, M. P.; Nevado, C.; Cárdenas, D. J.; Echavarren, A. M. *J. Am. Chem. Soc.* **2001**, *123*, 10511−10520.

(3) (a) Diver, S. T.; Giessent, A. J. *Chem. Rev.* **2004**, *104*, 1317−1382. (b) Mori, M. *Topics in Organometallic Chemistry*; Fürstner, A., Ed.; Springer-Verlag: Berlin, 1998; Vol. 1, p 133−154. (c) Fürstner, A. *Angew. Chem., Int. Ed.* **2000**, *39*, 3012−3043. (d) Poulsen, C. S.; Madsen, R. *Synthesis* **2003**, 1−18.

(4) (a) Trost, B. M.; M. J. Krische, M. J. *Synlett* **1998**, 1−16. (b) Trost, B. M.; Krische, M. J. *J. Am. Chem. Soc.* **1999**, *121*, 6131−6141. (c) Takayama, Y.; Okamoto, S.; Sato, F. *J. Am. Chem. Soc.* **1999**, *121*, 3559−3560. (d) Trost, B. M.; Toste, F. D. *J. Am. Chem. Soc.* **2000**, *122*, 714−715. (e) Trost, B. M.; Pedregal, C. *J. Am. Chem. Soc.* **1992**, *114*, 7292−7294. (f) Lei, A.; Waldkirch, J. P.; He, M.; Zhang, X. *Angew. Chem., Int. Ed.* **2002**, *41*, 4526−4529.

(5) (a) Mainetti, E.; Mouries, V.; Fensterbank, L.; Malacria, M.; Marco-Contelles, J. *Angew. Chem., Int. Ed.* **2002**, *41*, 2132−2135. (b) Anjum, S.; Marco-Contelles, J. *Tetrahedron* **2005**, *61*, 4793−4803.

(6) (a) Kakiuchi, F.; Yamauchi, M.; Chatani, N.; Murai, S. *Chem. Lett.* **1996**, 111−112. (b) Thalji, R. K.; Ahrendt, K. A.; Bergman, R. G.; Ellman, J. A. *J. Am. Chem. Soc.* **2001**, *123*, 9692−9693. (c) Boele, M. D. K.; van Strijdonck, G. P. F.; de Vries, A. H. M.; Kamer, P. C. J.; de Vries, J. G.; Leeuwen, P. W. N. M. *J. Am. Chem. Soc.* **2002**, *124*, 1586−1587. (d) Baran, P. S.; Corey, E. J. *J. Am. Chem. Soc.* **2002**, *124*, 7904−7905. (e) For a review on transition metal-catalyzed arylation of alkynes, see: Nevado, C.; Echavarren, A. M. *Synthesis* **2005**, 167−182.

(7) (a) Fürstner, A.; Mamane, V. *J. Org. Chem.* **2002**, *67*, 6264−6267. (b) Fürstner, A.; Mamane, V. *Chem. Commun.* **2003**, 2112−2113. (c) Mamane, V.; Hannen, P.; Fürstner, A. *Chem. Eur. J.* **2004**, *10*, 4556−4575.

10.1021/om0605332 CCC: $33.50 © 2006 American Chemical Society
Publication on Web 08/09/2006

Scheme 2

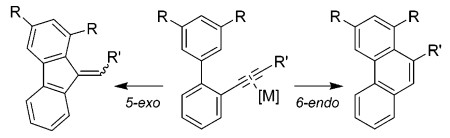

III I II

Experimental data reported by Fürstner et al (Scheme 2).[a]

R	R'	Catalyst (M)	II	III	Yield (%)
Me	Me	$PtCl_2$	100	0	89
Me	COOMe	$PtCl_2$	5	95	
OMe	H	$PtCl_2$	95	5	76
OMe	H	$GaCl_3$	96	4	53
OMe	H	$InCl_3$	44	56	44
OMe	H	$AuCl_3$	97	3	95

a In toluene, at 80ºC.

Scheme 3

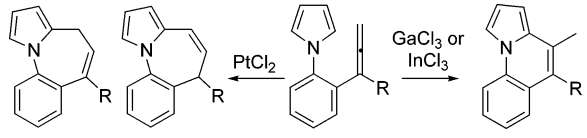

VI VII IV V

R = H, Me

Scheme 4

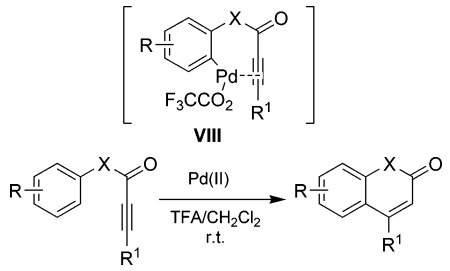

VIII

Diverse mechanistic proposals have been formulated in the last decade for the hydroarylation of alkynes, depending on the catalyst system. Fujiwara's group has described the Pt(II)- and Pd(II)-catalyzed regio- and stereoselective *trans*-hydroarylation of alkynes. They proposed the involvement of σ-aryl-metala-complexes **VIII**, formed through electrophilic metalation of aromatic C−H bonds (Scheme 4), followed by *trans*-addition across the alkyne.[9] Related C−H bond activation catalyzed by metal complexes has also been reported by Kobuke[10] and Trost.[11] However, recent mechanistic studies based on kinetic isotope effects with deuterated arene suggest that the reaction proceeds via electrophilic aromatic substitution.[12]

Sames et al. have developed an intramolecular hydroarylation methodology based on $PtCl_4$ in CH_2Cl_2 to form chromene, coumarin, and dihidroquinoline scaffolds from arene-yne compounds.[13] They have proposed that the cyclization proceeds through an alkyne activation−electrophilic substitution pathway rather than via Claisen rearrangement or arene metalation routes.[14]

Although in the past silver and mercuric salts have been known to mediate the cyclization of propargylic aryl ethers,[15] there are only a few reports on the use of these systems in the synthesis of polyarenes. In this sense, Nishizawa et al. have developed the cycloisomerization of aryl-alkynes catalyzed by Hg(II).[16] Hashmi et al. have described the $AuCl_3$-catalyzed intramolecular reaction of alkyne and furan to provide phenol,[17] a transformation also mediated less efficiently by transition metals with a d^8 configuration.[18] Recently, He and Shi have shown a Au(III)-based hydroarylation of alkynes under mild and solvent-free conditions.[19] They suggest a direct metalation of the arene to form an arylgold(III) intermediate, in analogy with the proposal by Hashmi, which could add to the alkyne to yield the final product.

Reetz and Sommer reported hydroarylation of alkynes catalyzed by Au(III)/Ag(I) systems, proposing that Au(III) likely works as a Lewis acid to increase the electrophilicity of the alkyne.[20] In this regard, Murai et al. have described the Ru- and Pt-mediated intramolecular couplings of alkynes with electron-rich arenes[21a] and also suggested that the transition metal complex acts as a Lewis acid, promoting the arene nucleophilic attack to the coordinated alkyne,[22,23] following a Friedel−Crafts-type mechanism (Scheme 5). On the basis of the hard and soft acid and base principle, they cleverly confirmed an improved electrophilic alkyne activation by Ga(III).[21b,24]

For Au- and Pt-catalyzed reactions, isotope experiments[17a,18] and the intramolecular cyclization of internal alkynes (Table 1)[7c] discard a mechanism via formation of a metal vinylidene

(8) (a) Soriano, E.; Ballesteros, P.; Marco-Contelles, J. *J. Org. Chem.* **2004**, *69*, 8018−8023. (b) Soriano, E.; Marco-Contelles, J. *Chem. Eur. J.* **2005**, *11*, 521−533. (c) Soriano, E.; Ballesteros, P.; Marco-Contelles, J. *Organometallics* **2005**, *24*, 3172−3181. (d) Soriano, E.; Ballesteros, P.; Marco-Contelles, J. *Organometallics* **2005**, *24*, 3182−3191. (e) Soriano, E.; Marco-Contelles, J. *J. Org. Chem.* **2005**, *70*, 9345−9353. (f) Marco-Contelles, J.; Soriano, E. *THEOCHEM* **2006**, *761*, 45−51.

(9) (a) Jia, C. G.; Piao, D. G.; Oyamada, J. Z.; Lu, W. J.; Kitamura, T.; Fujiwara, Y. *Science* **2000**, *287*, 1992−1995. (b) Jia, C.; Lu, W.; Oyamada, J.; Kitamura, T.;. Matsuda, K.; Irie, M.; Fujiwara, Y. *J. Am. Chem. Soc.* **2000**, *122*, 7252−7263. (c) Jia, C.; Piao, D.; Kitamura, T.; Fujiwara Y. *J. Org. Chem.* **2000**, *65*, 7516−7522.

(10) Kokubo, K.; Matsumasa, K.; Nomura, M. *J. Org. Chem.* **1997**, *62*, 4564.

(11) Trost, B. M.; Toste F. D. *J. Am. Chem. Soc.* **1996**, *118*, 6305−6306.

(12) Tunge, J. A.; Foresee, L. N. *Organometallics* **2005**, *24*, 6440−6444.

(13) (a) Pastine, S. J.; Youn, S. W.; Sames, D. *Org. Lett.* **2003**, *5*, 1055−1058. (b) Pastine, S. J.; Youn, S. W.; Sames, D. *Tetrahedron* **2003**, *59*, 8859−8868.

(14) The high efficiency and scope of this protocol as compared to $PtCl_2$ and the Fujiwara system ($Pd(OAc)_2$) has been proposed to be due to the higher electrophilicity (higher oxidation state of the metal center) and to the greater solubility of the catalyst in organic solvents.

(15) (a) Koch-Pomeranz, U.; Hansen, H.-J.; Schmid, H. *Helv. Chim. Acta* **1973**, *56*, 2981−3004. (b) Larock, R. C.; Harrison, L. W. *J. Am. Chem. Soc.* **1984**, *106*, 4218−4227.

(16) Nishizawa, M.; Takao, H.; Yadav, V. K.; Imagawa, H.; Sugihara, T. *Org. Lett.* **2003**, *5*, 4563−4565.

(17) (a) Hashmi, A. S. K.; Rudolph, M.; Weyrauch, J. P.; Wölfle, M.; Frey, W.; Bats J. W. *Angew. Chem., Int. Ed.* **2005**, *44*, 2798−2801. (b) Hashmi, A. S. K.; Frost, T. M.; Bats, J. W. *J. Am. Chem. Soc.* **2000**, *122*, 11553−11554. (c) Hashmi, A. S. K.; Frost, T. M.; Bats, J. W. *Org. Lett.* **2001**, *3*, 3769−3771. (d) Hashmi, A. S. K.; Frost, T. M.; Bats, J. W. *Catal. Today* **2002**, *72*, 19−72. (e) Hashmi, A. S. K.; Ding, L.; Bats, J. W.; Fischer, P.; Frey, W. *Chem. Eur. J.* **2003**, *9*, 4339−4345. (f) Hashmi, A. S. K.; Weyrauch, J. P.; Rudolph, M.; Kurpejoviæ, E. *Angew. Chem., Int. Ed.* **2004**, *43*, 6545−6547.

(18) Martín-Matute, B.; Nevado, C.; Cárdenas, D. J.; Echavarren, A. M. *J. Am. Chem. Soc.* **2003**, *125*, 5757−5766.

(19) Shi, Z.; He, C. *J. Org. Chem.* **2004**, *69*, 3669−3671.

(20) Reetz, M. T.; Sommer, K. *Eur. J. Org. Chem.* **2003**, 3485−3496.

(21) (a) Chatani, N.; Inoue, H.; Ikeda, T.; Murai, S. *J. Org. Chem.* **2000**, *65*, 4913−4918. (b) Inoue, H.; Chatani, N.; Murai, S. *J. Org. Chem.* **2002**, *67*, 1414−1417.

(22) For reactions of alkynes, promoted by Lewis acids, with weak carbon nucleophiles, see: (a) Asao, N.; Matsukawa, Y.; Yamamoto, Y. *Chem. Commun.* **1996**, 1513−1514. (b) Imamura, K.; Yoshikawa, E.; Gevorgyan, V.; Yamamoto, Y. *J. Am. Chem. Soc.* **1998**, *120*, 5339−5340. (c) Imamura, K.; Yoshikawa, E.; Gevorgyan, V.; Yamamoto, Y. *J. Am. Chem. Soc.* **1998**, *120*, 13284. (d) Jung, I. N.; Yoo, B. R. *Synlett* **1999**, 519−528. (e) Asao, N.; Shimada, T.; Yamamoto, Y. *J. Am. Chem. Soc.* **1999**, *121*, 3797−3798. (f) Tsuchimoto, T.; Maeda, T.; Shirakawa, E.; Kawakami, Y. *Chem. Commun.* **2000**, 1573−1574.

(23) For electrophile-induced cyclization to polycyclic aromatics, see: (a) Goldfinger, M. B.; Crawford, K. B.; Swager, T. M. *J. Am. Chem. Soc.* **1997**, *119*, 4578−4593. (b) Magnus, P.; Mitchell, I. S. *Tetrahedron Lett.* **1998**, *39*, 4595.

Table 1. NPA Charges on the Reactant Complex and Optimized Structural Parameters along the Reaction Coordinate

		1	2	3	4	5	6
NPA charge on **a**	C_1	−0.288	−0.288	−0.294	+0.003	−0.170	−0.277
	C_2	+0.131	+0.132	+0.136	+0.068	+0.173	+0.129
	C_{1ar}	−0.072	−0.056	−0.098	−0.051	−0.062	−0.041
	C_{2ar}	−0.202	−0.233	−0.183	−0.220	−0.212	−0.271
distance (in Å)							
a	Pt−C_1	1.977	1.977	1.974	2.033	1.995	1.981
	Pt−C_2	2.464	2.467	2.504	2.222	2.291	2.432
TS_a	Pt−C_1	2.585	2.513	2.562	2.727	2.615	2.437
	Pt−C_2	1.963	1.977	1.960	1.960	1.961	1.988
	C_1−C_{1ar}	2.513	2.696	2.269	2.394	2.743	2.816
	C_1−C_{2ar}	2.148	2.248	2.710	2.141	2.256	2.343
b	Pt−C_2	1.872		1.875	1.876		
	C_1−C_{1ar}	1.540		1.537	1.549		
	C_1−C_{2ar}	1.566		1.582	1.577		
TS_b	Pt−C_2	1.930		1.933	1.943		
	C_1−C_{1ar}	2.294		2.313	2.328		
	C_1−C_{2ar}	1.595		1.597	1.619		
c	Pt−C_2	1.942	1.946	1.939	1.953	1.944	1.949
	C_1−C_{1ar}	2.547	2.551	2.541	2.577	2.559	2.553
	C_1−C_{2ar}	1.492	1.501	1.490	1.508	1.514	1.506
TS_e	Pt−C_1	1.928	1.935	1.926	1.960	1.936	1.943
	Pt−C_2	2.808	2.797	2.829	2.741	2.752	2.768
	C_2−C_{1ar}	2.586	2.603	2.572	2.514	2.612	2.653
	C_2−C_{2ar}	2.095	2.168	2.074	2.046	2.112	2.295
f	Pt−C_1	1.891	1.899	1.891	1.913	1.916	1.904
	C_2−C_{1ar}	2.401	2.409	2.397	2.407	2.404	2.414
	C_2−C_{2ar}	1.530	1.533	1.531	1.535	1.538	1.537

[a] In toluene, at 80 °C.

Scheme 5

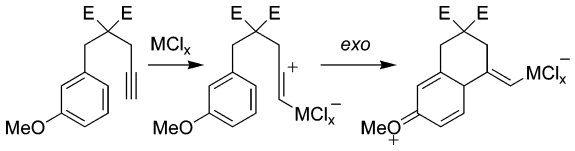

intermediate[25,26] followed by a 6π-electrocyclization. However, other metal complexes have been proven to catalyze the cyclization of aromatic alkynes via metal vinylidene intermediates. Thus, $W(CO)_5$(THF) promotes the electrocyclization of *o*-(iodoethynyl)styrenes to afford iodo-substituted naphthalene through tungsten-iodinated vinylidene as a key intermediate.[25d,e] Ru-based catalysts,[25a] such $RuCl_2$(*p*-cymenes)PPh_3 and cationic ruthenium complexes, also promote the cyclization of aromatic alkynes and enynes through this reaction pathway[25] and represent an efficient protocol for the aromatization of *o*-(ethynyl)phenyl ketones and aldehyde to give useful oxygen-containing compounds.[27] In this context, it is worth mentioning unexpected results reported by Fürstner in the same work,[7c] revealing a divergent behavior in the transformation of biaryls bearing a halo-alkyne moiety (**IX**) (Scheme 6), which in principle would be presumed to follow the same path as substrates **I**. Therefore, two clear and well-defined mechanistic schemes are proposed depending on the catalyst system.

Scheme 6

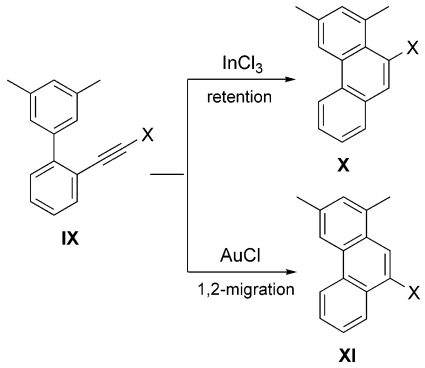

As has been summarized above, the currently assumed mechanism catalyzed by soft Lewis acids would follow a Friedel−Crafts alkenylation pathway.[28] The alkyne coordinates to the metal complex, to form an electrophilic π-alkyne complex or a vinyl cation,[7,29] which promotes the nucleophilic arene attack to generate a polycylic zwitterionic intermediate. Finally, this species evolves to the product by a formal [1,3]-H shift. On account of the observed rate dependence on the nucleophi-

(24) For Ga as Lewis acid for promoting addition of carbon nucleophiles to alkynes, see: (a) Arisawa, M.; Akamatsu, K.; Yamaguchi, M. *Org. Lett.* **2001**, *3*, 789−790. (b) Kido, Y.; Yonehara, F.; Yamaguchi, M. *Tetrahedron* **2001**, *57*, 827−833. (c) Yonehara, F.; Kido, Y.; Yamaguchi, M. *Chem. Commun.* **2000**, 1189−1190. (d) Yamaguchi, M.; Tsukagoshi, T.; Arisawa, M. *J. Am. Chem. Soc.* **1999**, *121*, 4074−4075. (e) Kido, Y.; Yamaguchi, M. *J. Org. Chem.* **1998**, *63*, 8086−8087. (f) Yamaguchi, M.; Sotokawa, T.; Hirama, M. *Chem. Commun.* **1997**, 743−744. (g) Yamaguchi, M.; Kido, Y.; Hayashi, A.; Hirama, M. *Angew. Chem., Int. Ed. Engl.* **1997**, *36*, 1313−1315.

(25) (a) Merlic, C. A.; Pauly, M. E. *J. Am. Chem. Soc.* **1996**, *118*, 11319−11320. (b) Sangu, K. Fuchibe, K.; Akiyama, T. *Org. Lett.* **2004**, *6*, 353−355. (c) Donovan, P. M.; Scott L. T. *J. Am. Chem. Soc.* **2004**, *126*, 3108−3112. (d) Maeyama, K. Iwasawa, N. *J. Am. Chem. Soc.* **1998**, *120*, 1928−1929. (e) Maeyama, K.; Iwasawa, N. *J. Org. Chem.* **1999**, *64*, 1344−1346. (f) Miura, T.; Iwasawa, N. *J. Am. Chem. Soc.* **2002**, *124*, 518−519. (g) O'Connor, J. M.; Friese, S. J.; Tichenor, M. *J. Am. Chem. Soc.* **2002**, *124*, 3506−3507. (h) Ohe, K.; Yokoi, T.; Miki, K.; Nishino, F.; Uemura, S. *J. Am. Chem. Soc.* **2002**, *124*, 526−527. (i) Iwasawa, N.; Maeyama, K.; Kusama, H. *Org. Lett.* **2001**, *3*, 3871−3873. (j) Kusama, H.; Yamabe, H.; Iwasawa, N. *Org. Lett.* **2002**, *4*, 2569−2571.

(26) Reviews on vinylidene complexes: (a) Bruneau, C.; Dixneuf, P. H. *Acc. Chem. Res.* **1999**, *32*, 311−323. (b) McDonald, F. E. *Chem.--Eur. J.* **1999**, *5*, 3103−3106. (c) Trost, B. M.; Toste, F. D.; Pinkerton, A. B. *Chem. Rev.* **2001**, *101*, 2067−2096.

(27) (a) Iwasawa, N.; Shido, M.; Kusama, H. *J. Am. Chem. Soc.* **2001**, *123*, 5814−5815. (b) Iwasawa, N.; Shido, M.; Kusama, H. *J. Am. Chem. Soc.* **2000**, 122, 10226. (c) Asao, N.; Takahashi, K.; Lee, S.; Kasahara, T.; Yamamoto, Y. *J. Am. Chem. Soc.* **2002**, *124*, 12650−12651. (d) Miki, K.; Nishino, F.; Ohe, K.; Uemura, S. *J. Am. Chem. Soc.* **2002**, *124*, 5260−5261.

(28) Dankwardt, J. W. *Tetrahedron Lett.* **2001**, *42*, 5809−5812.

(29) Pilette, D.; Moreau, S.; Le Bozec, H.; Dixneuf, P. H.; Corrigan, J. F.; Carty, A. J. *J. Chem. Soc., Chem. Commun.* **1994**, 409−410.

Chart 1

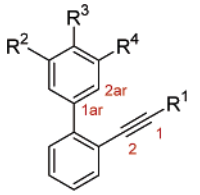

1: $R^1 = R^2 = R^3 = R^4 = H$
2: $R^1 = R^3 = R^4 = H$; $R^2 = OCH_3$
3: $R^1 = R^2 = R^4 = H$; $R^3 = OCH_3$
4: $R^3 = H$; $R^1 = R^2 = R^4 = CH_3$
5: $R^2 = R^3 = R^4 = H$; $R^1 = COOCH_3$
6: $R^1 = R^3 = H$; $R^2 = R^4 = OCH_3$

licity of the aromatic ring (i.e., electron-donating aromatic substituents favors the hydroarylation),[21b] it has been presumed that the first step is rate-limiting.

On the other hand, it has been extensively demonstrated by theoretical computations that divergent cycloisomerizations of enynes catalyzed by electrophilic transition metal complexes show a common mechanistic scheme[8a,c−e] and take place through the initial formation of metal cyclopropyl carbenes via an *exo*- or *endo*-cyclization pathway.[30] A partial theoretical study by Echavarren et al. on the intramolecular hydroarylation of 4- and 3-(butyn-3-yl)phenol suggests that both cyclopropanation and Friedel−Crafts pathways are feasible and similar in energy, thus giving an ambiguous resolution about the actual mechanism.[31] Moreover, they only analyzed the Pt(II)-catalyzed reaction, assuming that qualitatively similar results are obtained with Au(I) and Au(III) in the study on the cyclization of simple enynes. Nevertheless, our present results disagree with their proposals and reveal new conclusions regarding both the full reaction pathways and the influence of the catalyst system on the evolution of the key intermediate species.

In addition, to the best of our knowledge, we also report herein the first theoretical study of the mechanism and factors governing the regioselectivity on the hydroarylation of allenes mediated by a metal complex.

2. Results and Discussion

2.1. Cycloisomerization of *ortho*-Alkenyl Biphenyl Derivatives. First, we analyzed the intramolecular arene cyclization with alkyne promoted by different catalyst systems. Moreover, to gain insights into the influence of the arene substituents, we initially studied the biphenyl derivative **1** (Chart 1) as a model precursor, although it was not included in the experimental evaluation.[7c]

For the $PtCl_2$-catalyzed process, we have located a η^2-reactant complex **1a** formed by π-coordination of **1** to the metal complex (Pt−C_1 = 1.977 Å, Pt−C_2 = 2.464 Å; see Table 1), which may undergo a 6-*endo-dig* or a 5-*exo-dig* cyclization (Scheme 7).

The 6-*endo-dig* process proceeds through $\mathbf{TS_a1}$, which evolves to the cyclopropyl-platinum carbene intermediate **1b** (Pt−C_2 = 1.872 Å). The highly asynchronous transition structure (C_1−C_{1ar} = 2.513 Å, C_1−C_{2ar} = 2.148 Å) is 14.16 kcal mol^{-1} higher in energy than the reactant complex, and formation of the intermediate **1b** is exothermic (−5.81 kcal mol^{-1}) (Figure 1 and Table 2).

1b may evolve to the Wheland-type intermediate **1c** (Figure 1) by opening of the cyclopropane bond C_1−C_{1ar}. This step takes place through $\mathbf{TS_b1}$, which clearly shows a cleaved C_1−C_{1ar} bond (2.294 Å). The formation of the intermediate **1c** from the cyclopropyl platinum carbene **1b** is slightly endothermic (+0.42 kcal mol^{-1}) and involves an energy barrier of 12.00 kcal mol^{-1} (6.19 kcal mol^{-1} from **1a**). The altered bond lengths in the arene and the bond angles of the *ipso* carbon C_{2ar} in the intermediate **1c** clearly indicate the sp^3 hybridization, providing evidence for the full σ-character of this species, similar to those described experimentally in electrophilic aromatic substitution.[32]

Then, a formal [1,3]-H shift should lead to the final phenanthrene structure **e**. Since these reactions were performed, as usual, in an aprotic solvent (toluene), the proton migration cannot take place though an intermolecular solvent-mediated route. Therefore, we suggest a stepwise pathway via two consecutive [1,2]-H shift steps. Accordingly, we have characterized two transition structures, $\mathbf{TS_c1}$ and $\mathbf{TS_d1}$, connected by the intermediate **1d** (Figure 1), as IRC calculations confirm. The proton is located between C_{2ar} and C_1 (C_{2ar}−H = 1.179 Å, C_1−H = 1.555 Å) and C_1 and C_2 (C_1−H = 1.465 Å, C_2−H = 1.244 Å), respectively, for $\mathbf{TS_c1}$ and $\mathbf{TS_d1}$. As expected, the first [1,2]-H shift step is highly favored from both kinetic (energy barrier of +1.09 kcal mol^{-1}) and thermodynamic perspectives (highly exothermic, −38.11 kcal mol^{-1}), since it recovers the arene aromaticity without geometric strain. The final 1,2-H migration proceeds with an energy barrier of 23.66 kcal mol^{-1} (−19.84 kcal mol^{-1} below the reactant complex **1a**), a higher value than those computed for the same step in the cycloisomerization of 1,6- and 1,5-enynes bearing a propargylic heteroatom (17.62 and 18.93 kcal mol^{-1}, respectively),[8a,e] probably because the lone pair at the heteroatom promotes a [1,2]-H shift. Overall, the reaction is highly exothermic by −47.67 kcal mol^{-1}, which suggests the irreversible character of the catalyzed intramolecular process.

On the other hand, a 5-*exo-dig* cyclization can also take place. Contrarily to the 6-*endo* process, the nucleophilic attack to the internal alkyne carbon directly leads to the Friedel−Crafts-type intermediate **1f** via $\mathbf{TS_e1}$ (C_2−C_{2ar} = 2.095 Å), and an analogous cyclopropyl-Pt carbene is not observed along the energy profile, probably due to the high strain of a fused bicyclo[2.1.0]pentane framework (Figure 2). This step is slightly less exothermic (−5.12 kcal mol^{-1}) than the 6-*endo* path and proceeds with a lower activation energy (10.92 kcal mol^{-1}). The kinetic preference for the 5-*exo-dig* cyclization is comparable to that observed for linear enynes[8,33] and correlates with the computed NPA charges at C_1 (−0.288) and C_2 (+0.131) on the reactant complex **1a**. As for the *endo* route, two consecutive [1,2]-H shift steps would yield the final adduct. This stepwise [1,3]-H process takes place through $\mathbf{TS_f1}$ (C_{2ar}−H = 1.247, C_2−H = 1.380 Å) and $\mathbf{TS_g1}$ (C_2−H = 1.345, C_1−H = 1.323 Å), involving energy barriers of 9.86 and 10.17 kcal mol^{-1}, respectively. The global reaction is also highly exotermic, the fluorene skeleton **1h** being about 12 mol^{-1} less stable than phenanthrene **1e**.

According to this mechanism, electron-donating arene substituents should favor the hydroarylation process via both 5-*exo* and 6-*endo* routes. Thus, the effects of a methoxy group at the *meta* (**2**, Chart 1) or *para* position (**3**, Chart 1) of the biaryl connecting atom C_{1ar} have been evaluated.

As expected, the *meta*-substituent increases the charge at C_{2ar} on the reactant complex **2a** (Table 1). Remarkably, the *endo-dig* cyclization follows a Friedel−Crafts-type mechanism, affording the Wheland intermediate **2c**, while a cyclopropyl intermediate is not observed. This unanticipated result is probably caused by the reduced nucleophilicity at C_{1ar} (Table 1). As for the unsubstituted precursor **1**, the 5-*exo-dig* cyclization directly affords the zwitterionic intermediate **2f**. In contrast, the

(30) Echavarren, A. M.; Nevado, C. *Chem. Soc. Rev.* **2004**, *33*, 431−436.
(31) Nevado, C.; Echavarren, A. M. *Chem. Eur. J.* **2005**, *11*, 3155−3164.
(32) Hubig, S. M.; Kochi, J. K. *J. Org. Chem.* **2000**, *65*, 6807−6818.
(33) Nevado, C.; Cárdenas, D. J.; Echavarren, A. M. *Chem. Eur. J.* **2003**, *9*, 2627−2635.

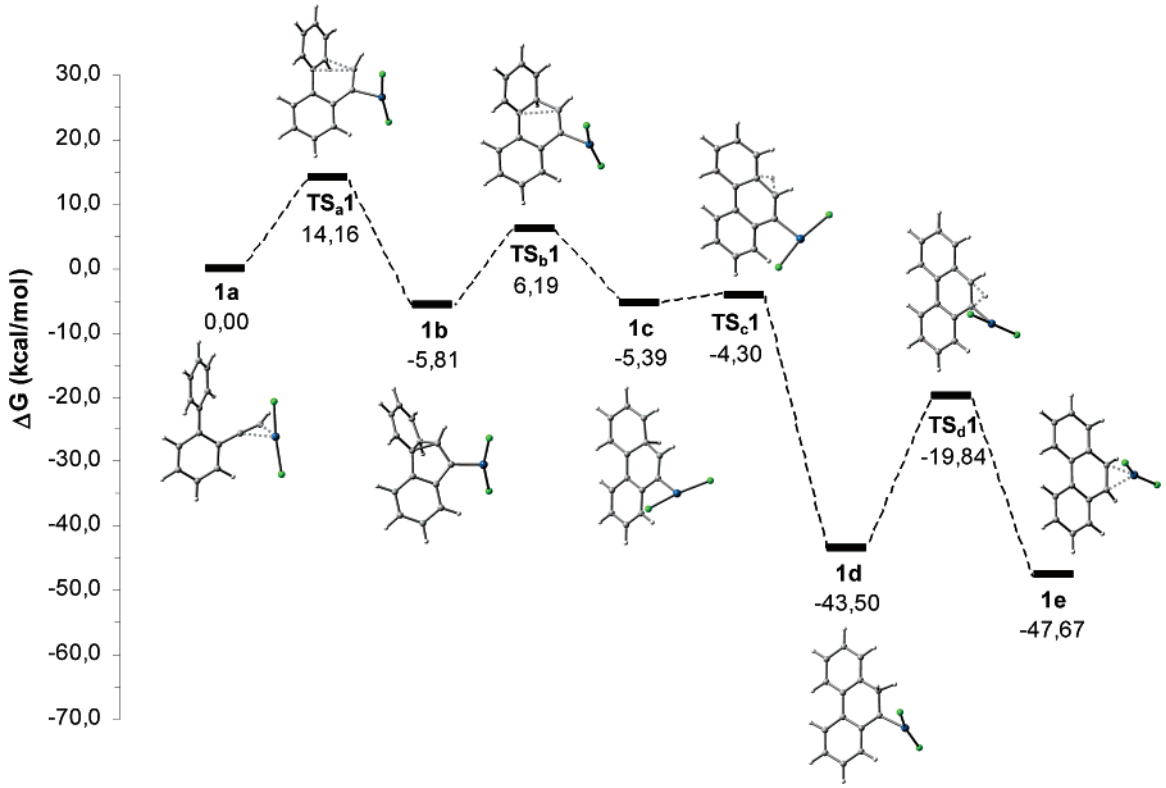

Figure 1. Computed reaction free-energy profile in solution (toluene) for the $PtCl_2$-catalyzed hydroarylation of alkyne **1** following an *endo-dig* cyclization mode.

Scheme 7

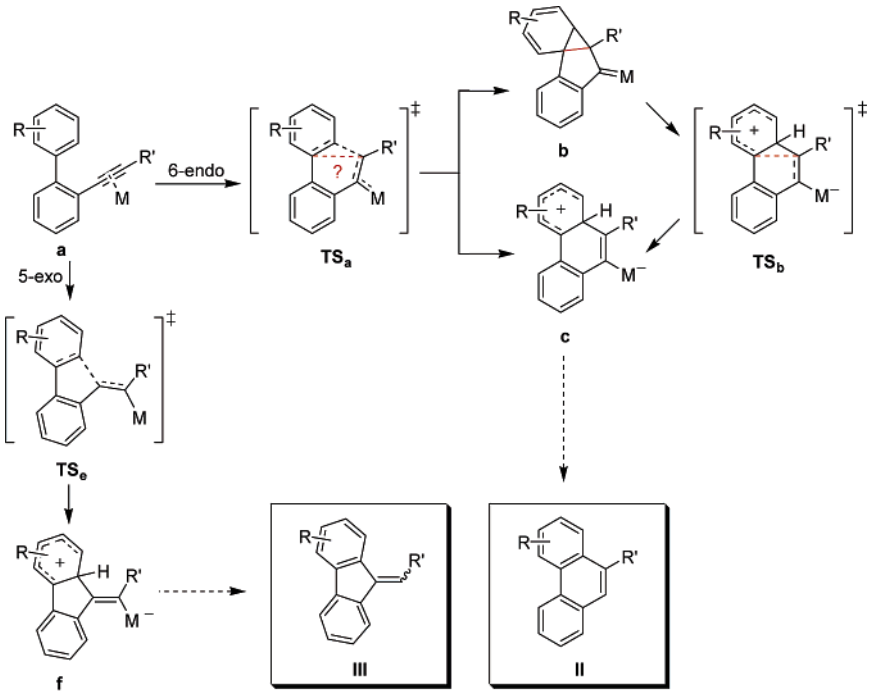

Scheme 7

endo-cyclization for the *para*-substituted precursor **3a** gives rise to the cyclopropylmetallacarbene **3b** as intermediate structure. The enhanced nucleophilicity at C_{1ar}, due to the electron-donor group at the *para* site, probably induces the stabilization of the cyclopropyl intermediate. This transformation takes place through the concerted $\mathbf{TS_a3}$, which shows that an orthogonal disposition of the arene planes allows a stronger interaction of the alkyne carbon C_1 with C_{1ar} (2.269 Å) than with C_{2ar} (2.709 Å). This high asynchronicity highlights the effects of the nature and position of the aromatic substituent on the reaction path when a tether connecting both reactive moieties is long enough. **3b** may evolve to the Wheland-type structure by C−C cyclopropane bond cleavage, through $\mathbf{TS_b3}$ ($C_1-C_{1ar} = 2.313$ Å), as has been described above for precursor **1**.

Comparing the series **1**−**3**, the cyclizations for **2** and **3** show earlier transition states than those for **1**, as can be deduced from

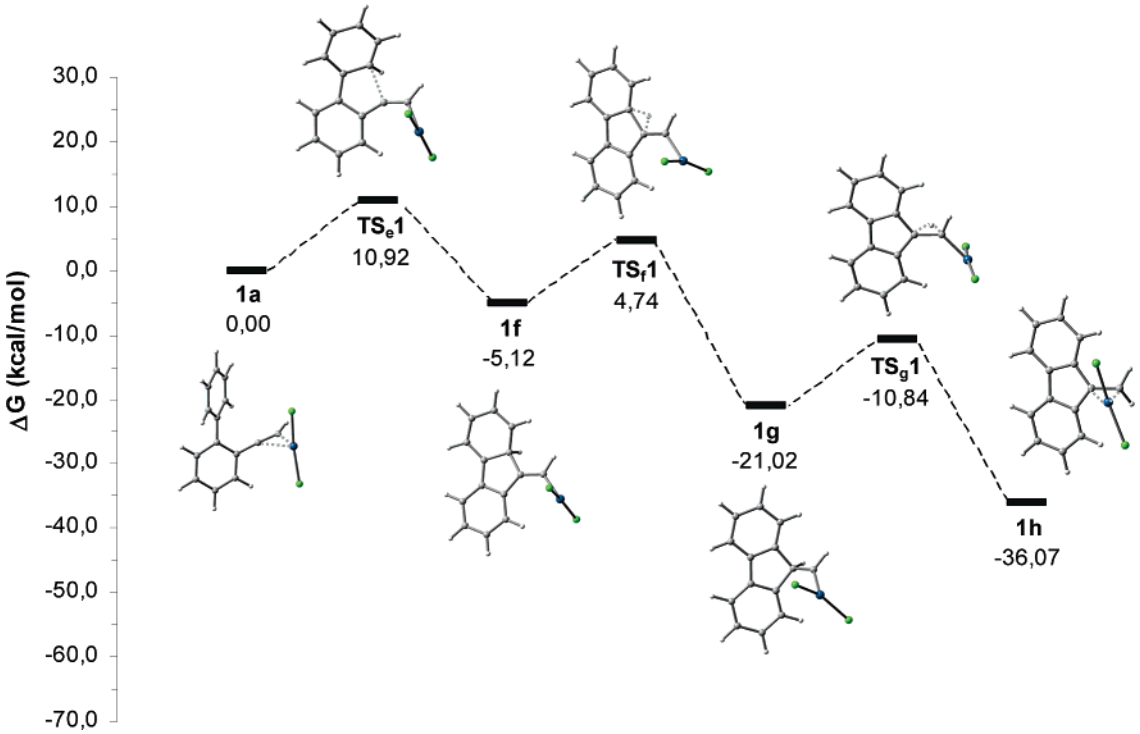

Figure 2. Computed reaction free-energy profile in solution (toluene) for the $PtCl_2$-catalyzed hydroarylation of alkyne **1** following an *exo-dig* cyclization mode.

Table 2. Relative Free Energy in Toluene (kcal mol^{-1}) for the *endo*- and *exo*-Cyclization Mode of Alkynes 1−6 (see Chart 1)

	1	2	3	4	5	6
a	0.00	0.00	0.00	0.00	0.00	0.00
TS$_a$	14.16	11.09	12.85	14.40	17.66	6.50
b	−5.81	*a*	−5.99	1.86	*a*	*a*
TS$_b$	6.19	*a*	7.68	8.85	*a*	*a*
c	−5.39	−13.39	−4.96	2.84	−4.00	−21.19
TS$_e$	10.92	10.08	12.12	18.79	14.36	8.35
f	−5.12	−13.07	−4.72	−0.62	−4.63	−20.82

[a] A cyclopropyl intermediate was not found.

the incipient bond distances in Table 1. Energy results reveal that they are kinetically more favorable than for the unsubstituted derivative **1** (Table 2) due to the enhanced nucleophilicity of the arene entity. Moreover, the cycloisomerization of **2**, bearing an electron-donating group at the *para* site with respect to the new C_1-C_{2ar} bond, shows the lowest activation energy, for both the *endo*- and *exo*-cyclization paths, whereas **2c** presents the highest stability of the tricyclic intermediates of type **c**.

Later, we focused on the biphenyl precursor **4**, bearing, in addition, an internal alkyne group. In this case, the alkyne carbon atoms display similar NPA charges (on **4a**), so the prevalent cyclization mode should be governed mainly by steric effects. The electrophilic attack of C_1 onto the aromatic ring leads, as for the unsubstituted compound **1**, to the concerted formation of cyclopropyl-Pt carbene **4b** through a less asymmetric transition structure, **TS$_a$4** ($C_1-C_{1ar} = 2.394$ Å, $C_1-C_{2ar} = 2.141$ Å, Table 1). This step is kinetically slightly less accessible than for the unsubstituted model **1** and less favored from a thermodynamic viewpoint (Table 2). The opening of the cyclopropane ring to form the Wheland-type structure relieves steric tension, and hence this step is faster than for **1** and **3** (6.99 vs 12.00 and 13.67 kcal mol^{-1}, respectively), although the intermediate **4c** is less stable than the reactant complex **4a**.

The transition state for the 5-*exo-dig* cyclization path, **TS$_e$4**, lies 18.79 kcal mol^{-1} above **4a** and 4.39 kcal mol^{-1} above **TS$_a$4**

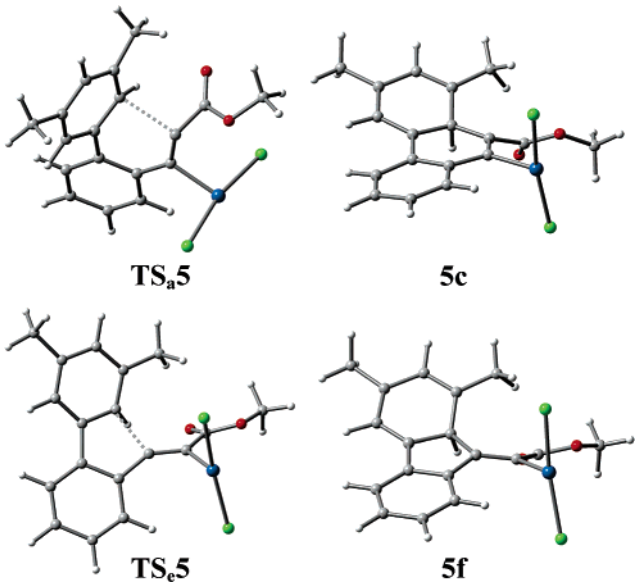

Figure 3. Optimized geometries for the *endo-dig* (top) and *exo-dig* cyclization (bottom) steps for precursor **5**.

for the *endo*-cyclization mode. The reduced NPA charge at C_2 on **4a** as compared to **1a**−**3a** and the steric hindrance from the C-sp^3 substituents (see Figure S1 in the Supporting Information) could account for the difficulty in reaching the transition state. These calculations agree with the experimental results reported by Fürstner,[7c] which revealed that formation of a 5-*exo* product from **4** was not observed. In sharp contrast, the electron-withdrawing ester group on the alkyne generates an opposite picture, since an increased electron-deficient character is observed at C_2 (NPA charges: $C_1 = -0.170$, $C_2 = +0.173$). This electronic effect should favor a 5-*exo* over a 6-*endo* process. Moreover, it must be expected that a strong steric hindrance between the substituents could inhibit the *endo* path (Figure 3). In accordance with these expectations, the computed results

Table 3. NPA Charges on the Reactant Complex and Optimized Structural Parameters

		$GaCl_3$		$InCl_3$		$AuCl_3$	
		1	**6**	**1**	**6**	**1**	**6**
NPA charge on **a**							
	C_1	−0.531	−0.537	−0.481	−0.489	−0.438	−0.426
	C_2	+0.202	+0.210	+0.154	+0.163	+0.193	+0.194
	C_{1ar}	−0.074	−0.046	−0.072	−0.045	−0.078	−0.045
	C_{2ar}	−0.208	−0.275	−0.210	−0.278	−0.198	−0.263
distance (in Å)							
a	$M-C_1$	2.203	2.194	2.410	2.396	2.136	2.135
	$M-C_2$	2.821	2.813	2.921	2.915	2.840	2.816
TS_a	$M-C_1$	2.790	2.699	2.941	2.864	2.757	2.596
	$M-C_2$	2.118	2.208	2.289	2.360	2.131	2.211
	C_1-C_{1ar}	2.584	2.824	2.593	2.775	2.595	2.944
	C_1-C_{2ar}	2.056	2.469	1.995	2.355	2.219	2.595
c	$M-C_2$	2.034	2.024	2.209	2.195	2.055	2.054
	C_1-C_{2ar}	1.500	1.517	1.504	1.521	1.497	1.512
TS_e	$M-C_1$	2.068	2.083	2.241	2.254	2.074	2.091
	$M-C_2$	2.990	2.948	3.152	3.110	2.948	2.927
	C_2-C_{1ar}	2.522	2.596	2.511	2.580	2.545	2.634
	C_2-C_{2ar}	1.944	2.163	1.910	2.120	2.028	2.270
f	$M-C_1$	2.020	2.010	2.196	2.182	2.020	2.024
	C_2-C_{2ar}	1.550	1.558	1.555	1.562	1.538	1.545

indicate that the *exo*-cyclization proceeds with a lower activation energy than the *endo* path (14.36 vs 17.66 kcal mol^{-1}, respectively). The successful orbital overlapping and charge donation needed to achieve the transition state **TS_a5** requires a C_1-C_{2ar} distance that, indeed, enhances the steric hindrance between the substituents (Figure 3). This acute steric effect could account for the high energy barrier for the *endo* mode. Additionally, as expected from the structural effects, both cyclization routes are kinetically less accessible than for other precursors. These observations are supported by the experimental results (*exo*:*endo* = 95:5).[7c]

The opposed regioselectivity was experimentally found for the substrate **6** (*exo*:*endo* = 5:95). In this case, a parallel reaction path to the precursor **2** can be envisaged. In fact, both cyclization modes analogously have been found to follow a Friedel−Crafts-type mechanism, through the early transition states **TS_a6** (for the *endo* path, C_1-C_{2ar} 2.343 Å) and **TS_e6** (for the *exo* path, C_2-C_{2ar} 2.295 Å). The formation of the vinylic metal intermediates takes place with lower energy barriers, 6.50 kcal mol^{-1} for the *endo* and 8.35 kcal mol^{-1} for the *exo* route. Interestingly, these values contrast with those found for the related precursors **2** and **3**, where the *exo*-cyclization mode was slightly favored from a kinetic point of view. For **6**, the reversed regioselectivity may be due to steric effects from the second methoxy group, since the aryl group cannot overcome this unfavorable effect by rotation, as is supposed to occur for **2**.

In summary, the intramolecular hydroarylation of biphenyl precursors **1**−**6** promoted by $PtCl_2$ may proceed via 6-*endo* and 5-*exo*-*dig* cyclization pathways, where subtle steric and electronic factors control not only the regioselectivity but the kind of intermediates involved in the reaction pathway. Thus, for the 6-*endo* path, i.e., if the tether connecting the reactive units is long enough, the reaction may follow a Friedel−Crafts alkenylation manifold to form the Wheland intermediate or may proceed through a concerted cyclopropanation route to yield a Pt-carbene as intermediate structure, which evolves to the Wheland intermediate by cyclopropane bond cleavage. Therefore, both direct and stepwise paths are *closely related* and governed by electronic factors. For precursors with a high nucleophilic C_{1ar} position or with an enhanced electrophilic character on the terminal alkyne carbon C_1, it is possible to locate a cyclopropyl intermediate as stable structure, by C_1-C_{1ar} bond formation, which may converge to the Wheland intermediate in a further step by cyclopropane bond cleavage. On the contrary, for precursors bearing weak nucleophile and electrophile units, this structure would probably be too unstable to be characterized as a stationary point on the reaction energy profile. In fact, the energy results for the cyclopropyl intermediate (for **1**, **3**, and **4**) indicate that this structure is more stable than the Wheland key intermediate. Interestingly, geometry optimization of the hypothetical intermediate of type **b** for precursor **2** reveals less stability than **2c** (by 5 kcal mol^{-1}). So, the stability of intermediate **b** as compared with **c** provides an interesting clue for the prediction of the actual reaction pathway. This observation sheds light on the mechanistic controversy of the cyclization step unresolved by the work by Echavarren et al.[31]

Once the effects of the arene and alkyne substituents were evaluated, we next analyzed the ability of other electrophilic metal complexes to promote these cycloisomerizations, such as $GaCl_3$, $InCl_3$, and $AuCl_3$, as was reported by Fürstner.[7c] Gold is a "soft" transition metal that shows high electrophilic affinity for "soft" functional groups, such as π-acids such as alkynes, and can also act as a Lewis acid for the activation of electrophiles,[34] in analogy with $GaCl_3$ and $InCl_3$ complexes.[21b,35,36] In addition, like $PtCl_2$, gold(III)-catalyzed cycloisomerizations of enynes have been suggested to proceed via formation of metal cyclopropyl carbene complexes.[33]

Because a different reaction pathway has been observed for the Pt(II)-catalyzed 6-*endo* process depending on the aromatic ring substituents, we have carried out the analysis for precursors **1** and **6** to gain deeper insights into the role of the catalyst.

The π-coordination of the alkyne to the metal center Ga(III) and In(III) affords a slipped η^1- rather than a η^2-complex (Table 3), probably in order to reduce unfavorable interactions with the aryl π-cloud, showing tetragonal coordination around the metal. This coordination mode has been reported for different

(34) (a) For a review of gold-catalyzed reactions, see: Hashmi, A. S. K. *Gold Bull.* **2004**, *37*, 51−65. (b) Arcadi, A. Di Giuseppe, S. *Curr. Org. Chem.* **2004**, *8*, 795−812. (c) Dyker, G. *Angew. Chem., Int. Ed.* **2000**, *39*, 4237−4239.

(35) Amemiya, R.; Yamaguchi, M. *Eur. J. Org. Chem.* **2005**, *24*, 5145−5150.

(36) For recent examples of use of $InCl_3$ as catalyst in organic synthesis: (a) Cook, G. R.; Hayashi R. *Org. Lett.* **2006**, *8*, 1045−1048. (b) Fringuelli, F.; Pizzo, F.; Tortoioli, S.; Vaccaro, L. *Org. Lett.* **2005**, *7*, 4411−4414. (c) Das, S. K.; Reddy, K. A.; Narasimha, R.; Krovvidi, V. L.; Mukkanti, K. *Carbohydr. Res.* **2005**, *340*, 1387−1392. (d) Jiang, N.; Li, C. J. *Chem. Commun.* **2004**, 394−395.

Table 4. Relative Free Energy in Toluene (kcal mol^{-1}) for the *endo*- and *exo*-Cyclization Mode of Alkynes 1 and 6 Catalyzed by $GaCl_3$, $InCl_3$, and $AuCl_3$

	$GaCl_3$		$InCl_3$		$AuCl_3$	
	1	**6**	**1**	**6**	**1**	**6**
a	0.00	0.00	0.00	0.00	0.00	0.00
TS_a	18.34	11.57	19.18	11.61	14.53	8.63
c	1.93	−12.95	5.64	−10.12	−3.61	−19.54
TS_e	17.05	12.85	19.08	11.11	12.36	10.47
f	8.44	−7.54	11.98	−8.83	−2.37	−16.46

Ga and In complexes.[37] Furthermore, the pertinent transition structures for the cyclization steps assuming alternative square-planar coordination could not be located. In contrast, the effective Au(III) complex exhibits a square-planar complex upon alkyne coordination, which can also be better described as a slipped η^1-complex.

The calculations reveal that none of the metal complexes promote the *endo* pathway through the formation of cyclopropylmetallacarbenes as intermediate structures. Instead, the electrophilic attack of the activated alkyne carbon C_1 or C_2 onto the arene results in the direct formation of the Wheland-type intermediates **c** and **f** via a Friedel−Crafts alkenylation pathway. An interesting hint was observed from the $AuCl_3$-catalyzed *endo-dig* cyclization of **3**, as it evolved to a spiro framework by single formation of C_1-C_{1ar} bond (not shown). To gain further insights, we also performed calculations on the *endo*-cyclization catalyzed by a cationic gold(I) complex $[Au(PR_3)]^+$, which has been proven very reactive and selective for the cyclizations of enynes under mild conditions.[38] It has been postulated that it probably involves cyclopropyl gold carbene as intermediates in the cyclization of simple enynes.[39] Our results reveal the same reaction paths as $AuCl_3$ for the promoted *endo*-cyclization of **1**, **3**, and **6**, with no formation of such intermediate (not shown). Hence, our results indicate that despite Au(III) (and Au(I)) complexes frequently behaving as Pt(II)-based catalysts, they share a different mechanistic picture for the *endo*-cyclization of aryl-alkynes. Caution must be exercised in extrapolating reaction pathways, even when dealing with related processes.

The *endo*-cyclization transition state **TS_a1** for the group 13 complexes and the *exo*-cyclization transition states **TS_e1** and **TS_e6** for all the catalyst systems appear later than those observed for the same Pt(II) process (Table 3), whereas **TS_a6** is earlier.

Taking into account the computed energy results (Table 4), the hydroarylation of the unsubstituted precursor **1** catalyzed by transition metal complexes shows a kinetic preference for the *exo*-cyclization mode, while the Ga(III) and In(III) complexes give rise to similar activation energy values for both routes and higher than those for Au(III) and Pt(II) halides. Moreover, the formation of the vinylic metal intermediates **c** and **f** promoted by these Lewis acids is endothermic, thus suggesting a low ability for **1** to cyclize under these conditions.

Scheme 8

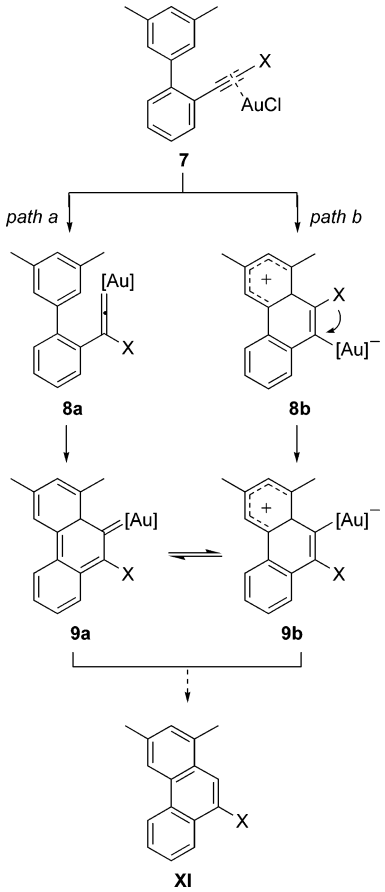

The improved nucleophilicity of the arene entity for the dimethoxy precursor **6** (see NPA charges, Table 3) results in a significant lowering of the ring closure activation barrier. It is noteworthy that formation of the Wheland-type intermediates is exothermic, the *endo*-adduct being more stable than the *exo*-adduct. As has been described for **1**, the Lewis acids $GaCl_3$ and $InCl_3$ display less favorable results, from both kinetic and thermodynamic points of view.

The $AuCl_3$-promoted cyclizations are not as exothermic as the Pt(II)-catalyzed reaction and have slightly higher activation energies, still favoring the *endo* process for **6**.

Overall, the results suggest that every catalyst follows the $PtCl_2$ trend, showing a kinetic and thermodynamic preference for the 6-*endo-dig* cyclization of **6**, but $InCl_3$, which leads to a slightly faster 5-*exo*-cyclization. In general, these observations agree with the experimental evidence. The results revealed for precursor **6** as compared with **1**, for a given catalyst, suggest that the methoxy substituent not only strongly favors the annulation due to electronic factors but may also play a steric role leading to a kinetic preference for the *endo*-cyclization. The divergent behavior for the $InCl_3$-catalyzed cycloisomerization showing no preference for the formation of a phenanthrene versus fluorene skeleton is unclear, although it might be due to subtle structural effects.[40]

The mechanistic scheme described above is in accordance with the widely accepted Friedel−Crafts-type pathway for the hydroarylation of alkynes mediated by an electrophilic metal complex. As we have noted in the Introduction, the intermediacy of metal vinylidene structures in these cyclizations has been

(37) (a) Sigl, M.; Schier, A.; Schmidbaur, H. *Eur. J. Inorg. Chem.* **1998**, 203-210. (b) Dhingra, S. S.; Kanatzidis, M. G. *Inorg. Chem.* **1993**, *32*, 1350−1362. (c) Trotter, J.; Einstein, F. W. B.; Tuck, D. G. *Acta Crystallogr., Sect. B* **1969**, *B25*, 603. (d) Johnson, B. F. G.; Walton, R. A. *Inorg. Chem.* **1966**, *5*, 49. (e) Wood, R. E.; Ritter, H. L. *J. Am. Chem. Soc.* **1952**, *74*, 1760−1763.

(38) (a) Ma, S.; Yu, S.; Gu, Z. *Angew. Chem., Int. Ed.* **2006**, *45*, 200−203. (b) Shi, X.; Gorin, D. J.; Toste, F. D. *J. Am. Chem. Soc.* **2005**, *127*, 5802−5803. (c) Zhang, L.; Kozmin, S. A. *J. Am. Chem. Soc.* **2005**, *127*, 6962−6963. (d) Luzung, M. R.; Markham, J. P.; Toste, F. D. *J. Am. Chem. Soc.* **2004**, *126*, 10858−10859 (e) V. Mamane, V.; Gress, T.; Krause, H.; Fürstner, A. *J. Am. Chem. Soc.* **2004**, *126*, 8654−8655.

(39) Nieto-Oberhuber, C.; Muñoz, M. P.; Buñuel, E.; Nevado, C.; Cárdenas, D. J.; Echavarren, A. M. *Angew. Chem., Int. Ed.* **2004**, *43*, 2402−2406.

(40) It could be argued that the related transition state (**TS_e6**) involves a short C_2-C_{2ar} distance and, hence, a close C_1-C_2-C angle, which indeed should induce a lower steric hindrance with the methoxy substituent.

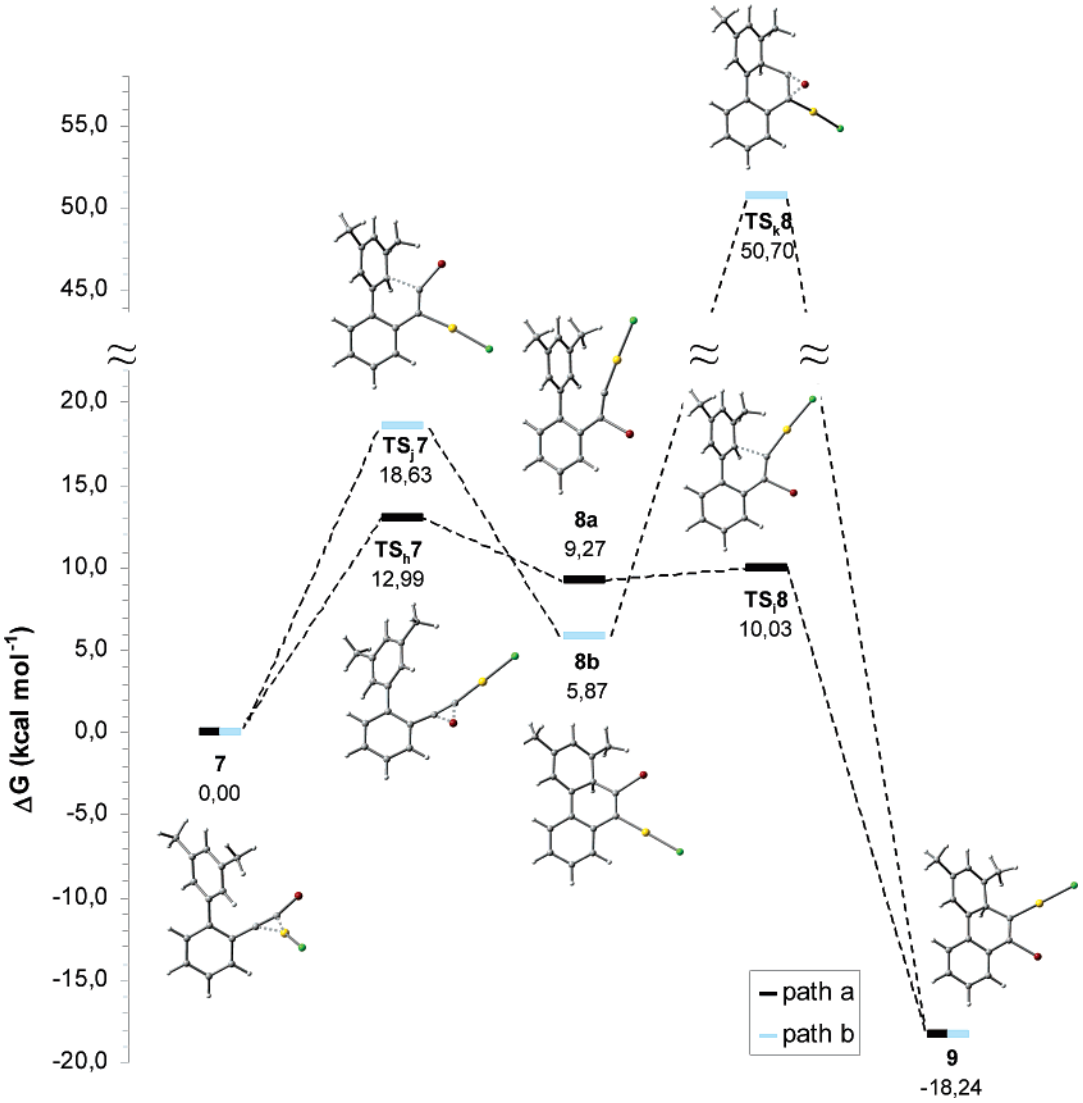

Figure 4. Free-energy profiles in solution (toluene) for the AuCl-catalyzed hydroarylation of halo-alkyne **7** following two plausible reaction pathways; see Scheme 8.

disregarded on the basis of the effective cyclization of internal alkynes and isotope studies.[7c,17a,18,28] However, the unanticipated formation of 9-halo-phenantrene **XI** from **IX**, upon exposure to catalytic amounts of AuCl (Scheme 6), points to the involvement of vinylidene intermediates, like those presumed in the cyclization of aromatic alkynes catalyzed by other transition metal complexes.[25,27]

The vinylidene structures might be formed by 1,2-halide shift[41] (Scheme 8, *path a*). On the basis of the mechanism suggested for the related complex $AuCl_3$, an alternative pathway through a common 6-*endo-dig* cyclization step followed by a 1,2-shift could also be envisaged (Scheme 8, *path b*). This mechanistic scheme has been proposed from studies of related transition metal-catalyzed cycloisomerizations.[8a,d,e]

The initial π-complex **7** undergoes a 1,2-halide shift to give the vinylidene species **8a**. This step takes place through **TS$_h$7** ($C_1-Br = 2.257$ Å, $C_2-Br = 2.195$ Å), a transition structure 12.99 kcal mol^{-1} above the reactant complex, and is endothermic by 9.27 kcal mol^{-1} (Figure 4). Then, the electrocyclization of **8a**, via the 6-*endo-dig* pathway, affords the tricyclic skeleton,[42] which ultimately should give rise to the 9-halophenanthrene through a formal 1,2-H shift. The electrocyclization transition structure **TS$_i$8** reveals the incipient formation of the C_1-C_{2ar} bond (2.175 Å). The minor steric hindrance between the catalyst and the arene may account for the favorable kinetic and thermodynamic results for this step, showing a very low energy barrier (0.76 kcal mol^{-1}) and being exothermic by about 27 kcal mol^{-1}.

The transformation of **7** through the alternative *path b* proceeds first through **TS$_j$7**, which displays structural parameters related to those found before ($C_1-C_{2ar} = 2.057$ Å), and leads to the Wheland-type intermediate. This Friedel−Crafts alkenylation step shows a higher activation barrier than that computed for *path a* (18.63 kcal mol^{-1}), likely related to the strong steric hindrance between the bulky halide atom and the C-sp^3 arene substituent in the reactive groups approach. From a thermodynamic point of view, this ring closure step appears favored (endothermic by 5.87 vs 9.27 kcal mol^{-1} for *path a*). The following 1,2-halide shift via **TS$_k$8** involves a very high energy barrier, about 45 kcal mol^{-1} (50.70 kcal mol^{-1} above **7**), probably caused by the large structural reorganization on a rather rigid skeleton.

(41) Shen, H.-C.; Pal, S.; Lian, J.-J.; Liu, R.-S. *J. Am. Chem. Soc.* **2003**, *125*, 15762−15763.

(42) The tricyclic intermediate is better described as **9b** than **9a**, as the bond length ($Au-C_1 = 2.025$ Å) and NBO analysis suggest (bond order $Au-C_1 = 0.611$).

Scheme 9

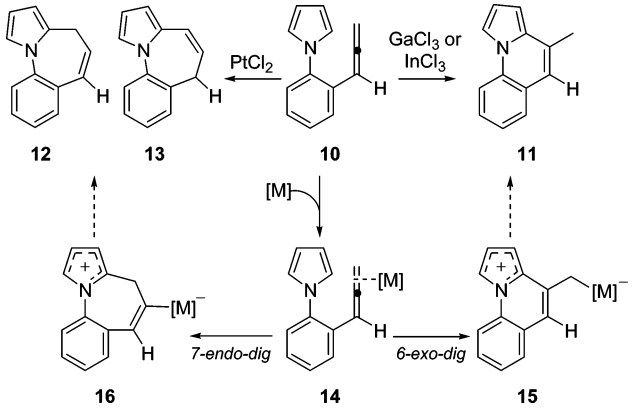

Hence, these results support *path a* as the operative mechanism, clearly favored over the alternative *path b*, which furthermore suggests a preferred formation of the 9- (**XI**) instead of the 10-halo-phenanthrene (**X**), since it would also take place through $\mathbf{TS_j7}$.

In sharp contrast, the Lewis acid $InCl_3$, which expectedly promotes the formation of 10-halo-phenanthrene with halide retention (**X**), leads to a different energy profile. Although indium-carbene complexes have been characterized,[43] the indium-carbene intermediate[44] and the pertinent transition structure analogue to $\mathbf{TS_h}$ could not be located after a thorough search, probably due to severe steric impediment between the ligands complex and the dimethylated arene. Instead, the system follows the *endo-dig* cyclization pathway, affording the vinylic indium intermediate through the transition state analogue to $\mathbf{TS_j}$ ($C_1-C_{2ar} = 2.079$ Å). This transformation is endothermic (by 5.44 kcal mol^{-1}) and involves an activation energy of 16.22 kcal mol^{-1}. These observations support a Friedel−Crafts-type mechanism for the $InCl_3$-promoted reaction and satisfactorily account for the divergent behavior depending on the chosen catalyst system.

2.2. Cyclization of Allenes. This flexible approach tolerates other unsaturated groups acting as an electrophilic entity, such as allenes. In this sense, the high reactivity of cumulated π-bonds is well-known.[45]

The experimental observations have revealed a well-defined regioselectivity that strongly depends on the catalyst. Thus, the allene precursor **10** afforded the phenanthrene framework **11** when Ga(III) and In(III) were employed as catalysts, whereas $PtCl_2$ gave rise to a mixture of isomeric pyrrolo-azepines **12** and **13** as major products (Scheme 9), which suggest a 6-*exo-dig* and 7-*endo-dig* cyclization pathway, respectively.[7c]

To shed light on the factors that control the regioselectivity, we have computed both cycloisomerization paths for every catalyst system. The results are graphically depicted in the Figure 5.

A 7-*endo-dig* cyclization should proceed from the allene moiety coordinated to the electrophilic complex, by means of the terminal π-bond for a proper activation, i.e., from reactant complex **14**. The cyclization to **16** (Scheme 9) is an exothermic transformation, $PtCl_2$ being the most favorable catalyst (Figure 5). The transition state $\mathbf{TS_m}$ lies about 10 kcal mol^{-1} above **14** for the Lewis acids, whereas it reduces to a half value for the late transition metal complex. The forming bond C−C shows slightly larger values (2.185, 2.431, and 2.285 Å, for $PtCl_2$, $GaCl_3$, and $IndCl_3$, respectively) than those observed above for the *endo*-cyclization of alkyne **1**. In summary, $PtCl_2$ gives to rise to the most favorable *endo*-cyclization mode from kinetic and thermodynamic viewpoints.

In the $PtCl_2$-promoted cycloisomerization, a higher yield for the formation of the pyrrolo-azepines **12** than for the isomeric form **13** was observed. However, according to our computed values, the former appears about 2 kcal mol^{-1} less stable than the latter. This result may point out a metal complex-mediated isomerization rather than a isomerization of the naked tricyclic adduct.

On the other hand, the *exo* route might take place by coordination of the terminal or the internal π-bond of the allene, since both modes may activate the central carbon. The reactant complex **14** (coordination of the terminal π-bond) gives rise to the tricyclic adduct **15** by attacking of the pyrrole to the activated central carbon of the allene. The formation of **15** is also exothermic. In this case, the Pt(II)-catalyzed reaction is moderately exothermic (−7.62 kcal mol^{-1}), and the Ga(III)- and In(III)-mediated steps are 3-fold more exothermic. The activation energy to reach the transition state $\mathbf{TS_l}$ is higher for $PtCl_2$ than for the trihalides. These results show the opposite trends to the *endo*-cyclization, suggesting a kinetic and thermodynamically favored *endo*-cyclization for the $PtCl_2$-mediated process and *exo*-cyclization for $GaCl_3$ and $InCl_3$. Amazingly, these findings are in good agreement with the regioselectivity observed experimentally.[7c]

The π-coordination of the internal double bond of the allene to the metal complex reveals structural restrictions and affords a less favorable energy profile (Figure 5). First, the *trans* halide arrangement in the $PtCl_2$ complex avoids the proper formation of the subsequent T-shaped Pt(II) complex **14′** by coordination of the allene, due to a strong steric repulsion between the ligands and the pyrrole moiety. On the contrary, the chloride atoms are far away in the Ga(III)- and In(III)-tetrahedral complexes **14′**. However, they are about 6 kcal mol^{-1} less stable than the reactant complex formed by coordination of the external double bond, **14**. These reactant complexes lead to the *exo*-cyclization adducts **15′** in a less exothermic step than that from **14** to **15**. In addition, the activation energy is significantly higher, so this alternative coordination mode should be discarded as operative in these transformations.

The striking catalyst-dependent regioselectivity can be rationalized in terms of electronic effects induced by structural factors on the reactant complex **14**.

The coordination to the terminal π-bond (**14**) results in a enhanced nucleophilic character of C_2 to the *exo*-attack compared with the coordination to the internal bond (Figure 6), consistent with the computed activation energy values. Moreover, Ga(III) and In(III) complexes induce a very low electrophilicity at C_1, which could explain the inhibition for the *endo*-cyclization route. This step is significantly less favored than for the $PtCl_2$ complex. The complex **14** exhibits an evident η^2-character for $PtCl_2$ ($Pt-C_1 = 2.101$ Å, $Pt-C_2 = 2.043$ Å), while the structures for $GaCl_3$ and $InCl_3$ resemble a weak η^1-hapticity, probably due to a steric hidrance between the metal complex ligands and the allene substituent at C_3 (Figure 7).

(43) (a) For an example of an In(III)-carbene, see: Cotgreave, J. H.; Colclough, D.; Kociok-Köhn, G.; Ruggiero, G.; Frost, C. G.; Weller, A. S. *Dalton Trans.* **2004**, 1519−1520. (b) For an example of an In(I)-carbene analogue, see: Hill, M. S.; Hitchcock, P. B. *Chem. Commun.* **2004**, 1818−1819.

(44) The energy minimization of the supposed In(III)-carbenic intermediate of type **8a** directly led to the formation of the 9-halo-phenanthrene framework (analogue to **9**).

(45) (a) Marshall, J. A. *Chem. Rev.* **2000**, *100*, 3163−3185. (b) Zimmer, R.; Dinesh, C. U.; Nandanan, E.; Khan, F. A. *Chem. Rev.* **2000**, *100*, 3067−3125. (c) Ma, S. *Acc. Chem. Res.* **2004**, *37*, 701−712. (d) Schuster, H. F.; Coppola, G. M. *Allenes in Organic Synthesis*; Wiley: New York, 1984.

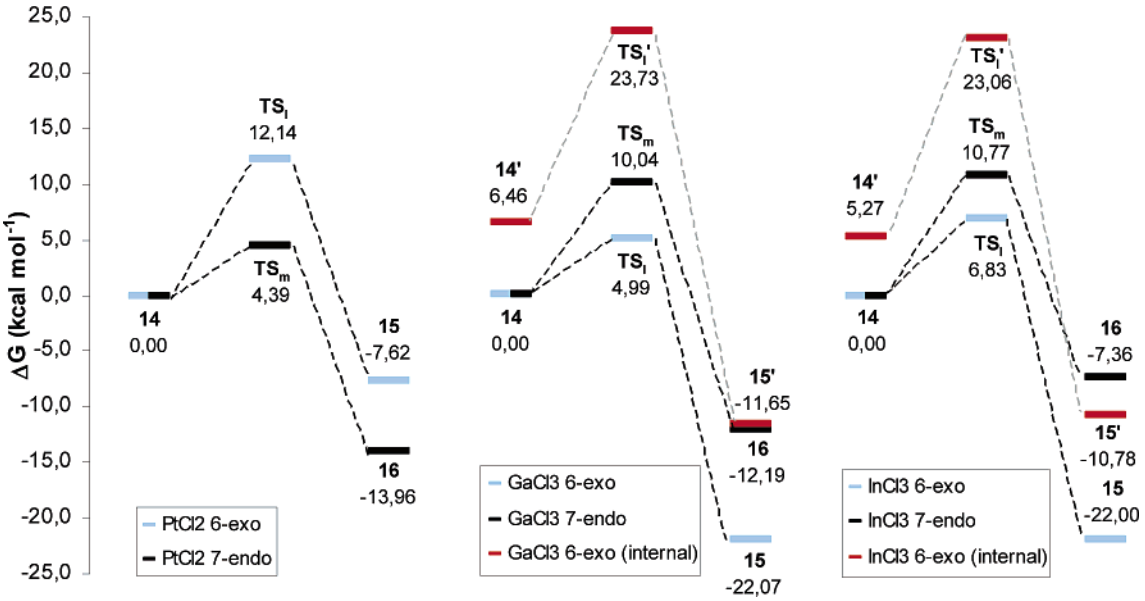

Figure 5. Reaction energy profiles for the catalyzed cyclization of allene **10** following an *endo*- and *exo*-route (through two plausible reaction pathways).

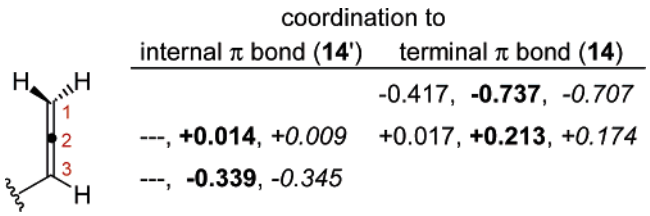

Figure 6. NPA charges at the allene carbons in the reactant complexes ($PtCl_2$ normal, $GaCl_3$ **bold**, $InCl_3$ *italic*) for the internal (**14′**) and terminal π-bond (**14**) coordinated complex.

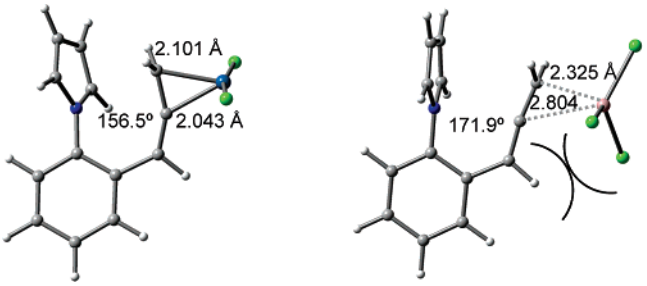

Figure 7. Optimized geometries for the reactant complexes **14** formed by coordination of the external π-bond of the allene to $PtCl_2$ (left) and $GaCl_3$ (right).

3. Conclusions

The intramolecular hydroarylation of aryl alkynes catalyzed by metal complexes may proceed via an *endo* and/or *exo-dig* cylization pathway, depending on the catalyst and on the precursor structure. Although these reactions have been seen to take place through a Friedel−Crafts-type alkenylation mechanism, the *endo-dig* cyclization promoted by $PtCl_2$ (but not $AuCl_3$) may involve a cyclopropylmetallacarbene as intermediate before the formation of the expected Wheland-type intermediate, i.e., the vinylic metal intermediate. This unusual electrophilic aromatic substitution reaction pathway has been observed for biaryls with a strongly nucleophilic arene entity (bearing a electron-donor substituent at the *para* position of the second C−C cyclopropyl new bond) or with a highly electrophilic C_1 alkyne carbon. Interestingly, this cyclopropyl metal intermediate must be a more stable species than the vinylic metal intermediate to be characterized as a local minimum along the reaction coordinate.

The *endo*/*exo* selectivity has been shown to deeply depend on the precursor substituents, where structural and electronic factors play a critical role. For dimethylated biaryl precursors bearing a haloalkyne, the steric hindrance in the Friedel−Crafts pathway forces the system to follow alternative and lower energy pathways, as through formation of metal vinylidene as key intermediate.

DFT computations have also revealed that the regioselectivity observed for the intramolecular cyclization of aryl allenes critically depends on subtle structural effects of the reactant complex. This species is preferably formed by coordination of the terminal π-bond of the allene rather than the internal π-bond. The metal complex ligands may involve steric hindrance with the substituent at the internal allene carbon C_3. This effect leads to an improved electrophilicity for the central allene carbon C_2 and a selective *exo-dig*-cyclization. On the contrary, the $PtCl_2$-reactant complex, with a *trans*-halide arrangement, lacks this effect and the reaction is preferentially guided to the unusual 7-*endo-dig* cyclization.

Computational Methods

Calculations have been carried out using the Gaussian03 program.[46] All the structures have been fully optimized at the DFT level by means of the B3LYP hybrid functional.[47] The standard 6-31G(d) basis set has been applied for all the atoms except metals Pt, Au, Ga, and In, which have been described by the LANL2DZ basis set,[48] where the innermost electrons are replaced by a relativistic ECP and the valence electrons are explicitly treated by a double-ζ basis set.

The optimized geometries were characterized by means of harmonic analysis, and the nature of the stationary points was determined according to the right number of negative eigenvalues of the Hessian matrix. The intrinsic reaction coordinate (IRC)

(46) Frisch, M. J., et al. *Gaussian 03*, Revision B.03; Gaussian, Inc.: Pittsburgh, PA, 2003.
(47) (a) Lee, C.; Yang, W.; Parr, R. *Phys. Rev. B* **1988**, *37*, 785−789. (b) Becke, A. *J. Chem. Phys.* **1993**, *98*, 5648−5652.
(48) Hay, P. J.; Wadt, W. R. *J. Chem. Phys.* **1985**, *82*, 270−283.

pathways[49a] from the transition structures have been carefully followed from every transition structure using a second-order integration method,[49b] to verify the expected connections of the first-order saddle points with the correct local minima found on the potential energy surface. Zero-point vibration energy (ZPVE) and thermal corrections (at 298 K, 1 atm) to the energy have been estimated on the basis of the frequency calculations at the optimization level and scaled by the recommended factor.

The solvation energies were calculated on the gas-phase optimized structures with the Polarizable Continuum Model, PCM,[50] as implemented in Gaussian 03, and using the UAKS radii.[51] A relative permittivity of 2.379 was assumed in the calculations to simulate toluene as the solvent experimentally used.

Natural bond orbital (NBO) analyses[52] have been performed by the module NBO v.3.1 implemented in Gaussian03 to evaluate the NPA atomic charges.

Acknowledgment. E.S. thanks Gobierno de La Rioja for a postdoctoral fellowship.

Supporting Information Available: Complete ref 46, one additional figure showing the transition structures $\mathbf{TS_a4}$ and $\mathbf{TS_e4}$, and atomic coordinates for the computed structures. This material is available free of charge via the Internet at http://pubs.acs.org.

OM0605332

(49) (a) Fukui, K. *Acc. Chem. Res.* **1981**, *14*, 363−368. (b) González, C.; Schlegel, H. B. *J. Phys. Chem.* **1990**, *94*, 5523−5527.

(50) (a) Tomasi, J.; Persico, M. *Chem. Rev.* **1994**, *94*, 2027−2094. (b) Cossi, M.; Scalmani, G.; Rega, N.; Barone, V. *J. Chem. Phys.* **2002**, *117*, 43−54.

(51) Barone, V.; Cossi, M. *J. Phys. Chem. A* **1998**, *102*, 1995−2001.

(52) (a) Reed, A. E.; Weinhold, F. *J. Chem. Phys.* **1983**, *78*, 4066−4073. (b) Reed, A. E.; Curtiss, L. A.; Weinhold, F. *Chem. Rev.* **1988**, *88*, 899−926.